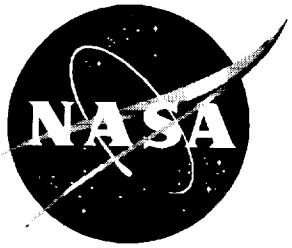

NASA Contractor Report 4578

Localized and Distributed Boundary-Layer Receptivity to Convected Unsteady Wake in Free Stream

Meelan Choudhari
High Technology Corporation • Hampton, Virginia

National Aeronautics and Space Administration
Langley Research Center • Hampton, Virginia 23681-0001

Prepared for Langley Research Center
under Contract NAS1-19299

April 1994

Localized and Distributed Boundary-Layer Receptivity to Convected Unsteady Wake in Free Stream

Meelan Choudhari
High Technology Corporation
Hampton, VA 23666

Abstract

Receptivity to a model convected disturbance in the presence of localized and distributed variations in wall geometry and wall-suction velocity is examined. The model free-stream disturbance corresponds to the time-harmonic wake of a vibrating ribbon that is placed at a suitable distance above the surface of a thin airfoil. The advantages of using this disturbance for experiments on receptivity to convected disturbances are outlined. A brief parametric study is presented for a flat-plate boundary layer. The study quantifies the effect of wake position as well as wake width; in addition, it should be helpful in the choice of an optimal setting for a controlled experiment of the above type, which the above parametric study shows as feasible.

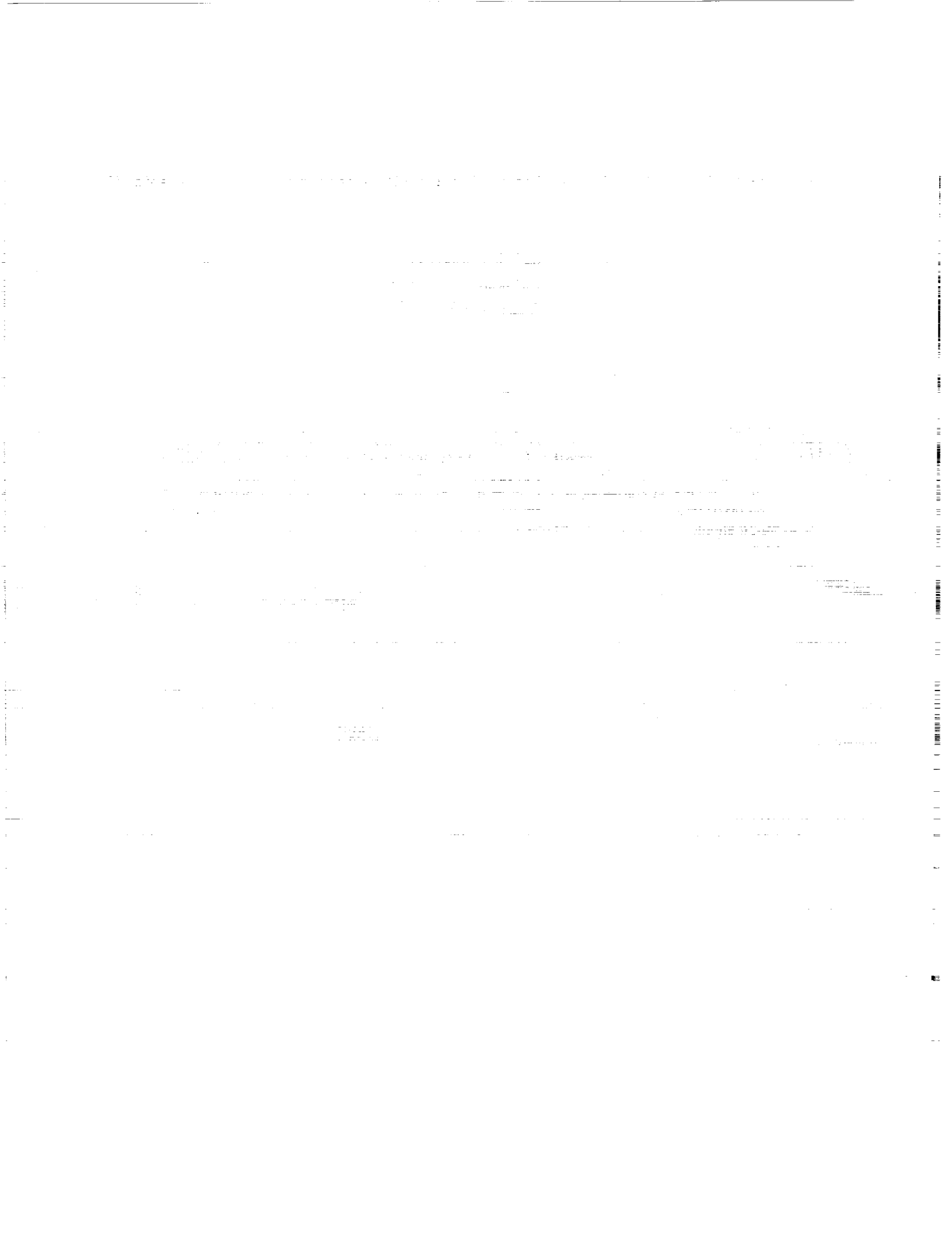

1 Introduction

The transition of boundary-layer flow from the laminar to a turbulent state is usually initiated by the excitation of linear instability waves, due to forcing from the external disturbance environment. A detailed understanding of this initial stage, which is known as boundary-layer receptivity [1, 2], is important for the prediction and control of the overall transition process. Therefore, accurate quantitative predictions are necessary for the different physical mechanisms that make the boundary layer *receptive* to each category of free-stream disturbance.

The receptivity mechanisms in low-speed flows were recently clarified in a series of seminal papers by Goldstein [3, 4]; see, also, the work of Zavol'skii et. al. [5], Ruban [6], and Fedorov [7], [8] in this respect. These authors showed that the receptivity is usually caused by relatively fast streamwise variations in the underlying mean flow. These variations may be caused by the boundary-layer growth in the leading-edge region [3], or by short-scale variations in surface boundary conditions, such as localized surface humps (or cavities) [3, 6], distributed surface waviness [5], or even laminar flow control (LFC) devices such as discrete suction strips [9]. Surface disturbances are particularly important in this regard, because they can occur in proximity to the region of instability amplification [4].

The work on boundary-layer receptivity so far has resulted in a substantial body of results that pertains to the receptivity to acoustic free-stream disturbances. See, for instance, the review article by Goldstein and Hultgren [10] and the relevant papers in refs. 11 and 12. In addition to the irrotational acoustic perturbations, the disturbance environment of a low-speed boundary layer includes vortical disturbances of various forms [13]: a. free-stream turbulence; b. unsteady wakes from upstream bodies; c. buoyant turbulent plumes in the atmosphere; and d. sheets, wakes, patches, strips, rings, or streets of vorticity that are convected at varying speeds. Disturbances of type (a–c) are usually convected at the local free-stream speed. In the linear approximation, these disturbances are decoupled from the acoustic fluctuations, except when boundary inhomogeneities or mean-flow variations occur. In regions that are sufficiently further removed from such scattering agents, the purely convected disturbances are expected to produce little fluctuation in the free-stream pressure. However, the convection speed of the disturbances from category d. is not necessarily equal to the local mean speed. Hence, these disturbances can induce nonzero pressure fluctuations everywhere, even at the linear order, and can thus be regarded as possessing elements common to both purely acoustic and purely convected disturbances. The receptivity to the above vortical disturbances has received relatively less attention so far, except

for the studies described in the remaining part of this section.

The problem of receptivity to free-stream turbulence is probably the most relevant one in practice, especially in the extrapolation of laboratory findings to flight environments. However, this problem is also the most complex one, as may be evidenced from the controlled experiments by Kendall [14]. For this reason, it seems useful to investigate the receptivity to simpler forms of convected free-stream disturbances. Although periodic vortex arrays [15] are relatively simple to analyze theoretically, they are difficult to produce in a controlled environment (Parekh et al. [16], Wlezien, private communication, 1993). One specific convected disturbance, which can be produced quite easily in a laboratory, is the wake of a vibrating ribbon that is placed outside the mean boundary layer at a suitable streamwise location. Receptivity experiments involving a convected-wake disturbance of this type were first conducted by Levchenko et al. [17] in which the convected nature of the wake disturbance was confirmed within the limitation of experimental errors. Later, Zavol'skii et al. [5] presented a brief calculation of the receptivity to an unsteady wake amid small-amplitude undulations on a flat-plate airfoil. In that case, the unsteady wake could excite an instability wave because the mean-flow perturbation from the surface undulations created a sharp tuning effect. Zavols'kii et al. showed that the interaction between the unsteady wake and the mean-flow perturbation was confined to the free-stream region of the wake, and that the resultant receptivity was significantly weaker than the receptivity for an acoustic disturbance that interacts with the surface waviness.

Conclusions similar to those of Zavol'skii et al. were subsequently obtained by Kerschen [18] and Crouch [19] in somewhat different contexts. Kerschen used a simple but elegant asymptotic theory to study the localized receptivity that is caused by the interaction between an isolated roughness element and an unsteady vortical gust with a sinusoidal distribution of velocity perturbations upstream of the airfoil. Kerschen then combined his results with those of Goldstein [4] and of Ruban [6] for localized acoustic receptivity to derive predictions for the surface-geometry-induced receptivity to a Karman vortex street with an arbitrary convection velocity. He found that a large increase in the amplitude of the generated instability wave is possible if the convection velocity differs significantly from the free-stream speed.

The receptivity to purely convected free-stream disturbances amid surface nonuniformities is relatively weak, so the receptivity related to leading-edge effects needs to be investigated. Heinrich *et al* [20] studied the receptivity to an unsteady sinusoidal gust near the leading edge of a sharp-edged

flat plate by using the framework of Goldstein [3]. A computational study of the receptivity to an unsteady-wake disturbance near a rounded leading edge was recently reported by Buter and Reed [21]. Parekh [22] performed experiments on the receptivity to a similar wake disturbance, but found little receptivity. The reasons for this finding have not been identified in a conclusive manner.

The objective of this paper is to further investigate the receptivity to a convected unsteady wake. We consider the receptivity caused by localized variations in surface geometry and in surface-suction velocity; our aim is to quantify the differences in receptivity for the two surface disturbances as well as the differences in each case with the analogous acoustic-receptivity mechanism. In addition to the relative ease in producing the convected-wake disturbance in a laboratory, using this model disturbance has the advantage that the associated receptivity via leading-edge effects can be minimized by suitably positioning the disturbance source within the free-stream region. Moreover, because the primary wake disturbance is localized to the free-stream region, it does not interfere with the measurement of the generated Tollmien-Schlichting (TS) wave, the mode shape of which has a global maximum close to the surface. As a result, the convected-wake model provides a potentially cleaner setting for the experimental verification of the theoretical predictions related to the localized receptivity to convected disturbances. Experimental measurements of similar receptivity processes for an acoustic free-stream disturbance have been conducted by Aizin and Polyakov [23], Saric et al. [24], and Wiegel and Wlezien [25] (see also the work of Wlezien et al. [26]), and a satisfactory agreement with a Goldstein-Ruban type theory has been found [27], [28], [29], [30] in each case. Although the explanation of Parekh's findings [22] is beyond the scope of this paper, we believe that the parametric study reported here will be helpful in designing an optimal setting for future experiments and may also provide a clue to understand the trends observed therein.

Toward the above-mentioned objectives, we use a finite-Reynolds-number adaptation of the original Goldstein-Ruban theory [4], [6]. A general description of this approach in the context of acoustic receptivity caused by local surface nonuniformities was given in reference [28], and additional details were provided in reference [29]. Therefore, only a brief sketch of the underlying analysis will be presented herein, with an emphasis on the issues that are specific to the convected nature of the free-stream disturbance.

2 Summary of the Analysis

As first shown in Refs. 4, 5, and 6, the receptivity due to a suitably weak, and spatially localized surface inhomogeneity (such as a roughness element) is the result of a scattering of the unsteady motion associated with the free-stream disturbance by the short-scale variations in the local mean flow that are induced by the surface inhomogeneity. Consider a thin, two-dimensional airfoil with a local disturbance on its surface in the form of a shallow roughness element or a local region of weak suction through the wall at a distance ℓ^* from the leading edge. We assume that the maximum perturbation in the surface height that is associated with the wall-geometry perturbation h_w^* is sufficiently small compared with the local displacement thickness δ^* of the unperturbed mean boundary layer; so the local mean-flow disturbance due to the roughness element can be treated as a small perturbation to the unperturbed mean flow. Analogously, the mean suction velocity V_w^* is assumed to be sufficiently small with respect to the local free-stream velocity U_∞^*. The two small parameters h_w^*/δ^* and V_w^*/U_∞^* are henceforth denoted $\epsilon_w^{(r)}$ and $\epsilon_w^{(s)}$, respectively. Also, the unsteady free-stream disturbance is assumed to be a time-harmonic wake that passes above the airfoil in the region just outside of the mean boundary layer. The amplitude of the wake, measured in terms of the maximum of the associated perturbation in the streamwise velocity, is taken to be small (i.e., $\epsilon_{wake} = u_{wake}^*/U_\infty^* << 1$) so that any nonlinear effects can be neglected in the calculation of the leading-order unsteady motion. Physically, this disturbance corresponds to a longitudinal array of vortices that is convected at the local free-stream velocity just outside the mean boundary layer.

By exploiting the presence of the two small parameters $\epsilon_w^{(j)}$ ($j = r$ or s) and ϵ_{wake} in the problem, we can expand the streamfunction $\psi^{(j)}$ within the local region in terms of the dual perturbation series

$$\psi^{(j)}(X,Y,t) = \psi_0(Y) + \epsilon_w^{(j)}\,\psi_w^{(j)}(X,Y) + \epsilon_{wake}\,\hat{\psi}_{wake}(Y)\,e^{i\omega(X-t)} + \epsilon_{wake}\,\epsilon_w^{(j)}\,\psi_{w,wake}^{(j)}(X,Y)\,e^{-i\omega t} + O(\epsilon_{wake}^2, {\epsilon_w^{(j)}}^2) \quad (1)$$

where the streamfunction $\psi^{(j)}$, the local coordinates along the streamwise X and wall-normal Y directions, the wake-frequency parameter ω, and the time t have been nondimensionalized by $U_\infty^*\delta^*$, δ^*, U_∞^*/δ^*, and δ^*/U_∞^*, respectively. The zeroeth order term ψ_0 corresponds to the unperturbed mean flow in the absence of disturbances both at the surface and in the free stream and is given simply by the mean boundary-layer profile at the location of the surface inhomogeneity (taken to be $X = 0$ herein) to the required level of accuracy. The leading-order mean-flow disturbance produced by the roughness

element or the suction strip is denoted $\psi_w^{(j)}(X,Y)$, with the superscript j set equal to 'r' in the former case and to 's' in the latter. The Fourier transform variables $\bar{\psi}_w^{(j)}(\alpha,Y)$, $(j = r,s)$ then satisfy the steady version of the Orr-Sommerfeld equation, subject to an inhomogeneous boundary condition corresponding to the specified distribution of the roughness geometry and/or suction velocity. (See reference [29] for details.)

The leading-order unsteady solution that corresponds to the $O(\epsilon_{wake})$ term in equation (1) is determined by the interaction between the free-stream disturbance and the unperturbed mean boundary layer. Because the unsteady wake is confined to a narrow region above the mean boundary layer, it produces negligible upwash at the airfoil. The only way the wake motion can be affected by the airfoil is through its interaction with the inviscid mean flow that the airfoil induces. We now utilize the thin-airfoil approximation, which implies that the local inviscid stream may be assumed sufficiently uniform so as to produce only a weak distortion of the unsteady vorticity associated with the wake. In other words, any pressure fluctuations produced from the wake-airfoil interaction are assumed insignificant to the local receptivity process. In practice, this approximation will be valid in most wind-tunnel experiments, which typically involve flat-plate models. To the leading order, the local unsteady motion then corresponds to the convection of the disturbance profile at the local free-stream velocity. For brevity, we have already anticipated this conclusion in the expansion of equation (1) by including the "convected phase" $\omega(X-t)$ in the exponent of the $O(\epsilon_{wake})$ term. The local profile of the associated streamfunction $\psi_{wake}(Y)$ is assumed to be known from computations that include a knowledge of the upstream disturbance, or from experiments such as those described in reference [17].

The term that is crucial for receptivity is, however, the $O(\epsilon_w^{(j)}\epsilon_{wake})$ term; it is produced from the scattering of the leading-order unsteady solution described above by the local mean-flow gradients induced by the inhomogeneity at the surface [5], [4]. The Fourier transform $\bar{\psi}_{w,wake}^{(j)}(\alpha,Y)$ of this term satisfies the inhomogeneous Orr-Sommerfeld equation

$$
\begin{aligned}
&-i\omega(D^2-\alpha^2)\bar{\psi}_{w,wake}^{(j)} + i\alpha\hat{\Psi}_0'(D^2-\alpha^2)\bar{\psi}_{w,wake}^{(j)} - i\alpha\hat{\Psi}_0'''\bar{\psi}_{w,wake}^{(j)} - \frac{1}{R_{\delta^*}}(D^2-\alpha^2)^2\bar{\psi}_{w,wake}^{(j)} \\
&\quad = \left[-i\alpha_{wake}\frac{d\bar{\psi}_w^{(j)}}{dY}(D^2-\alpha_{wake}^2)\hat{\psi}_{wake} + i\alpha_w\bar{\psi}_w^{(j)}D(D^2-\alpha_{wake}^2)\hat{\psi}_{wake}\right] \\
&\quad + \left\{-i\alpha_w\frac{d\hat{\psi}_{wake}}{dY}(D^2-\alpha_w^2)\bar{\psi}_w^{(j)} + i\alpha_{wake}\hat{\psi}_{wake}D(D^2-\alpha_w^2)\bar{\psi}_w^{(j)}\right\} \quad , \qquad (2a)
\end{aligned}
$$

along with homogeneous boundary conditions at the surface and at infinity. In equation (2a), the

symmetric definition of Fourier transform has been used. The streamwise wavenumbers of the free-stream and surface perturbations are given by

$$\alpha_{wake} = \omega, \quad \text{and} \quad \alpha_w = \alpha - \alpha_{wake} \ , \tag{2b}$$

respectively; the operator D as well as the primes are used to denote derivatives with respect to the wall-normal coordinate Y and the Reynolds number R_{δ^*} is based on U^*_∞ and δ^*. The source terms on the right of equation (2a) arise from the nonlinear interaction between the two first-order perturbations $\psi^{(j)}_w$ and $\hat{\psi}_{wake}$. The first set of source terms that is enclosed by the brackets is due to the convection of the unsteady free-stream vorticity $(D^2-\alpha^2_{wake})\hat{\psi}_{wake}$ by the local mean-flow disturbance $\bar{\psi}^{(j)}_w$. Similarly, the second set of source terms (enclosed by the curly braces) arises from the convection of the mean disturbance vorticity $(D^2 - \alpha^2_w)\bar{\psi}^{(j)}_w$ by the unsteady perturbation $\hat{\psi}_{wake}$ associated with the wake. Because of the two-dimensional nature of the problem, the effects of vorticity tilting are absent from these source terms.

It is possible to further simplify the source terms in equation (2a) by exploiting the fact that the mean disturbance vorticity is nearly zero in the free-stream region (which implies that the contribution from the second set of source terms is negligible) and by taking advantage of the disparity between the streamwise and the wall-normal length scales of the convected-wake disturbance (which implies that the leading contribution comes from the first term inside the brackets, i.e., one that involves $\frac{d^2\hat{\psi}_{wake}}{dY^2}$). However, these simplifications will be not be introduced here, so equation (2a) is also valid for a more general convected disturbance. The part of the unsteady scattered field $\psi^{(j)}_{w,wake}$ that corresponds to the unstable TS wave can be isolated as the residue contribution to the inverse Fourier integral from the simple-pole singularity in the Fourier transform $\bar{\psi}_{w,wake}$ at the local instability wavenumber $\alpha = \alpha_{ins}(\omega, R_{\delta^*})$. The dimensional streamwise velocity fluctuation $u^{(j)*}_{ins}$ associated with this instability wave can be expressed as

$$u^{(j)*}_{ins}(X, Y, t) = C^{(j)}\ u^*_{wake}\ E_u(Y;\ \omega, R_{\delta^*})\ \exp\left[i(\alpha_{ins}X - \omega t)\right] \ , \tag{3a}$$

where E_u denotes the instability-wave eigenfunction for the streamwise velocity perturbation, which is normalized for a maximum magnitude of unity across the boundary layer. The "local coupling coefficient" [4] $C^{(j)}$ in equation (3a) represents the ratio of the local amplitude of the generated instability wave to u^*_{wake}, the amplitude of the free-stream disturbance. For the weak surface inhomogeneities

examined herein, this coupling coefficient is given by the product

$$C_u^{(j)} = \epsilon_w^{(j)}\ \bar{F}^{(j)}(\alpha_{ins} - \alpha_{wake})\ \Lambda_{wake}^{(j)}(\omega, R_{\delta^*})\ . \tag{3b}$$

The factor $\bar{F}(\alpha_{ins} - \alpha_{wake})$ denotes the Fourier transform of the local geometry of the surface inhomogeneity (e.g., surface-height or suction-velocity distributions), evaluated at the complex wavenumber $(\alpha_{ins} - \alpha_{wake})$. This particular Fourier component "tunes" the free-stream disturbance of wavenumber α_{wake} ($\equiv \omega$ for the convected wake) to the wavenumber α_{ins} of the instability wave. The factor $\Lambda_{wake}^{(j)}(\omega, R_{\delta^*})$, on the other hand, is independent of the local geometry and depends only on the particular combination of surface inhomogeneity and free-stream disturbance involved in the receptivity process. In view of the decomposition indicated in equation (3b), the receptivity caused by different combinations of surface and free-stream disturbances can be studied and/or compared just on the basis of their respective "efficiency functions" $\Lambda_{\cdot\cdot}^{(j)}$ without regard to the particular geometry.

With the knowledge of $\Lambda_{wake}^{(j)}$, the receptivity caused by nonlocal (i.e., distributed) surface nonuniformities can also be computed quite easily, as described in references [29] and [31]. One specific nonlocal distribution that is easily realized in a laboratory experiment corresponds to a periodic array of identical, compact surface nonuniformities [25]. The maximum receptivity is known to occur [5], [31] when the fundamental wavenumber of this distribution is close to the instability wave number at the lower branch station. Based on equation (18b) of reference [33], the ratio of the effective coupling coefficient in this case to that caused by a single nonuniformity of the same type is given by the expression

$$\frac{C_{u,\,array}^{(j)}}{C_u^{(j)}} = \frac{\alpha_{ins,\mathrm{lb}}}{\bar{F}^{(j)}(\alpha_{ins,\mathrm{lb}})\sqrt{i\pi\tilde{D}_\alpha}} \sum_{n=1}^{\infty} \bar{F}^{(j)}(n\alpha_{w,\mathrm{lb}}) \exp\left[-\frac{(n\alpha_{w,\mathrm{lb}} + \alpha_{wake,\mathrm{lb}} - \alpha_{ins,\mathrm{lb}})^2}{i\tilde{D}_\alpha}\right] \tag{4a}$$

where $\alpha_w(R_{\delta^*}) \equiv \alpha_w^* \delta^*(R_{\delta^*})$ denotes the fundamental wave number of the periodic distribution, and the factor

$$\tilde{D}_\alpha \equiv \left(\frac{R_{\delta^*}^2}{R_{\ell^*}}\right)_{\mathrm{lb}} D_\alpha \qquad \left[D_\alpha = (\alpha'_{ins,\mathrm{lb}} - \frac{\alpha_{ins,\mathrm{lb}}}{R_{\delta^*_{\mathrm{lb}}}})\right] \tag{4b}$$

is a measure of how rapidly the unsteady forcing (produced by the interacting free-stream and surface disturbances) becomes detuned with respect to the phase of the instability mode. The primes in equation (4b) denote differentiation with respect to R_{δ^*} and the subscript lb indicates evaluation at the lower branch location $R_{\delta^*} = R_{\delta^*_{\mathrm{lb}}}$. In applying the theory of reference [33] to derive equation (4a), we have assumed that the increase in wake thickness (due to viscous diffusion) is negligible over the

length scale of distributed receptivity. Because the latter length scale is asymptotically small (viz., of $O(R_{\ell_{1b}^*}^{-3/16}\ell^*)$), the above assumption is quite reasonable.

3 Results

For a parametric study based on the above theory, we choose the unperturbed mean flow ψ_0 to be the Blasius streamfunction that corresponds to the flow past a flat-plate airfoil. The receptivity to a convected-wake disturbance in this simple geometry was first studied by Levchenko and Kozlov [17] in their experiments. Zavol'skii et al. [5] investigated the distributed receptivity in the same configuration, but in the presence of a small-amplitude waviness in the plate surface. As quoted in this latter paper, the experimentally measured profile of the unsteady streamfunction $\psi_{wake}(Y)$ had been found approximately Gaussian. Therefore, following Zavol'skii *et al.* [5], we assume that $\psi_{wake}(Y)$ is given by

$$\psi_{wake}(Y) = \frac{i\omega_{wake}L}{2^{1/2}} \exp[-(Y - Y_c)^2/L^2 + 1/2] \tag{5}$$

where $Y = Y_c$ denotes the position of the centerline of the wake relative to the unperturbed airfoil surface and L denotes a characteristic width of the unsteady wake profile. Note that the profile in equation (5) has been normalized such that the maximum magnitude of the associated perturbation in the unsteady streamwise velocity is equal to unity.

3.1 Suction-induced receptivity

3.1.1 Comparison with acoustic receptivity

To compare the strength of wall-suction-induced receptivity for a convected-wake disturbance (given by equation (5)) to the strength of an analogous receptivity mechanism for an acoustic free-stream disturbance, we have shown a combined plot of the magnitudes of the respective efficiency functions $\Lambda^{(s)}_{wake}(f)$ and $\Lambda^{(s)}_{acoustic}(f)$ in figure 1. Here, the location of the suction strip has been assumed fixed at $R \equiv \sqrt{R_{\ell^*}} = R_{\delta^*}/1.7208 = 700$ in both cases while the frequency parameter $f \equiv \omega^*\nu^*/{U^*_\infty}^2$ is varied from $20\text{x}10^{-6}$ to $80\text{x}10^{-6}$. These parameter values are relevant in both laboratory and in-flight situations. The position of the wake centerline is assumed to be at $Y_c = 5.0$ and the wake width L is taken to be unity. These wake parameters are identical to those considered by Zavol'skii et al. [5] in their calculation of the receptivity caused by distributed surface waviness; the Reynolds number chosen

is close to the approximate design Reynolds number of 620 in the experiments of Wiegel and Wlezien [25].

In figure 1, the efficiency function $\Lambda^{(s)}_{wake}(f)$ has been magnified by 100 to fit both curves on the same plot. It is then immediately obvious that for a given suction velocity, the receptivity to a convected wake is generally weaker than the acoustic receptivity by a factor that is comparable to this magnification. In particular, at the lower branch frequency ($f = f_{lb} \approx 39 \times 10^{-6}$), the ratio $|\Lambda^{(s)}_{wake}|/\Lambda^{(s)}_{acoustic}|$ is close to 1/80. Let us assumes that the distribution of the wall-suction velocity is uniform across the width d of a suction strip, i.e., $F^{(s)}(X)$ corresponds to a top-hat distribution

$$F^{(s)}(X) = \mathcal{V}_w \quad |X| < -d/2; \quad F^{(s)}(X) = 1 \quad \text{otherwise.} \tag{6a}$$

Then, if the scaled suction rate $\mathcal{V}_w$ is kept constant as the strip width d is varied, it is easily shown that the maximum coupling coefficient at the above frequency corresponds to a strip width that is equal to

$$d = \pi/\alpha_{ins} \tag{6b}$$

(i.e., half of the local instability wavelength). Substituting equations (6a) and (6b) into equation (3) and setting $\epsilon^{(s)}_w = 2 \times 10^{-4}$ (which represents a reasonable level of suction for both LFC applications and is also expected to satisfy the linearized approximation utilized in the present theory), the maximum local coupling coefficient for a single suction strip is found to be only 2.9×10^{-4} when $f = 39 \times 10^{-6}$. Using the result in equation (4) in conjunction with the D_α values presented in figure 3 of reference [31], we find that the maximum value of the effective coupling coefficient for a periodic array of suction strips is 8.9 times larger than the coupling coefficient for a single strip. (In fact, the ratio of coupling coefficients in these two cases is nearly constant across a wide range of frequencies for the Blasius boundary layer.) The above increase is not sufficient to compensate for the weaker receptivity to a convected wake, so we conclude that the net receptivity of an entire suction-strip configuration to the convected wake in equation (5) is less strong as compared to the maximum acoustic receptivity due to a single suction strip. Recall that a significant reduction in receptivity was also observed by Kerschen [18] for vortical disturbances that are periodic in the wall-normal direction. These findings simply underscore the recent viewpoint that a simple, global indicator of the free-stream disturbance environment (such as the root-mean-square amplitude of the associated velocity fluctuations) is practically meaningless for even a crude estimate of the initial amplitudes of the instability waves in any given configuration. Therefore, the existing measurement techniques need improvement so that at least the decomposition

of the total disturbance intensity between its irrotational (*i.e.*, acoustic) and rotational (*i.e.*, vortical) components can be specified, if not the detailed spectra of frequency and orientation corresponding to each component.

An equally noteworthy feature of figure 1 is the different behaviour of the efficiency-function curves for the two types of free-stream disturbances. The acoustic efficiency function has its largest value in the range of very small frequencies and displays a nearly monotonic decay at larger values of f. In contrast, the efficiency function for the convected wake is nearly zero at small frequencies. It increases quite rapidly with f up to about the lower branch frequency $f \approx 39 \times 10^{-6}$; at larger frequencies, the increase in $|\Lambda^{(s)}_{wake}|$ is relatively slow. It is shown in section 3.1.2 that the shape of the $|\Lambda^{(s)}_{wake}(f)|$ curve depends on the values of the wake parameters Y_c and L and that for $Y_c > 5.0$ the magnitude of $\Lambda^{(s)}_{wake}$ begins to decrease after f becomes sufficiently large. However, the frequency parameter that corresponds to the peak value of $|\Lambda^{(s)}_{wake}|$ is usually close to $f = f_{\mathrm{lb}}$ in the parameter range considered here.

3.1.2 Influence of wake position

Figure 2 illustrates the influence of the wake-centerline position Y_c on $|\Lambda^{(s)}_{wake}|$. We have plotted the efficiency function magnitude for wake positions that vary from $Y_c = 5.0$ to 10.0, while the width and the profile of the wake as well as the suction-strip location, are held fixed at the same values as those in figure 1. As the wake moves further away from the edge of the mean boundary layer, the receptivity becomes increasingly weaker, especially at the higher frequencies. The reason for this decrease is twofold. First, the outward movement of the wake centerline is accompanied by a similar shift in the region of the wake interaction with the mean-flow disturbance $\psi^{(s)}_w$ that is produced by the suction strip. This shift results in a reduced effectiveness of the interaction because the efficiency of a given compact source in the free-stream region in producing an instability wave decreases at a rate proportional to $e^{-\alpha_{ins} Y_c}$ when the distance Y_c of the source from the surface is increased. (See, for instance, the work by Ryzhov [32], which examines a related model problem.)

The second cause that further enhances the decrease in $|\Lambda^{(s)}_{wake}|$ at large Y_c is related to the decreasing strength of the interaction itself when Y_c is increased. This decrease occurs because of an exponential decay in the amplitude of the relevant Fourier harmonic $\bar{\psi}^{(s)}_w(\alpha_w)$ ($\alpha_w \equiv \alpha_{ins} - \alpha_{wake}$) of the mean-flow disturbance. Recall from equation (3) that the receptivity is produced when the wake is scattered by

the Fourier component $\psi_w^{(s)}(\alpha_w)$ of the mean-flow disturbance, which corresponds to a (complex) wave number $\alpha_w = \alpha_{ins} - \alpha_{wake}$. The amplitude of $\bar{\psi}_w^{(s)}(\alpha_w, Y)$ in the narrow wake region can be shown to decresase exponentially with Y_c, at a rate that is proportional to $\exp[-\alpha_w Y_c]$.

Therefore, the effect of wake position on the efficiency function can be characterized by

$$\Lambda_{wake}^{(s)}(\omega, R_{\delta^*};\ Y_c) = \exp[-(\alpha_{ins} + \alpha_w)(Y_{c;ref} - Y_c)]\ \Lambda_{wake}^{(s)}(\omega, R_{\delta^*};\ Y_{c;ref}) \tag{6}$$

where the added subscript ref indicates some reference wake position. If the results plotted in figure 2 were normalized using equation (6), all the curves would collapse onto each other, which confirms the accuracy of the correlation in equation (6). Because the decay rate $\alpha_{ins} + \alpha_w$ in equation (6) is an increasing function of f, decrease in $|\Lambda_{wake}^{(s)}|$ with Y_c is especially pronounced at the higher values of f. (See fig. 2.) This nonuniform effect of Y_c on the efficiency-function magnitude leads to a qualitative change in the shape of the frequency-response curve as Y_c is increased. Specifically, as Y_c increases beyond 5.0, the $|\Lambda_{wake}^{(s)}|$ curve displays a maximum at a frequency that decreases with an increase in Y_c. For $Y_c < 10$, this frequency is somewhat smaller than the lower branch frequency ($f_{lb} \approx 39 \times 10^{-6}$).

3.1.3 Influence of wake width

For a given wake profile (eq. (5)) and a given maximum fluctuation in the streamwise velocity, the efficiency function magnitude correlates nearly with the square of the wake width L. This point is well illustrated by figure 3 where the magnitude of the normalized efficiency function $\Lambda_{wake}^{(s)}/L^2$ has been plotted for different values of L. Thus, the efficiency function magnitude for $L = 1.5$ is nearly 2.25 times larger than the corresponding value at $L = 1$ for any f. This correlation suggests that one of the primary reasons the wake-induced receptivity is weaker than the convected-gust receptivity [18] is probably the spatial compactness of the wake disturbance. (See, also, the comments following eq. (7) in sec. 3.2).

3.2 Wall-geometry induced receptivity

Let us now compare the efficiency functions for the wall-geometry induced receptivity for the convected-wake and acoustic free-stream disturbances. The magnitudes of these efficiency functions (viz., $\Lambda_{wake}^{(r)}$ and $\Lambda_{acoustic}^{(r)}$) are shown in figure 4 for $Y_c = 5.0$ and $L = 1.0$. Similar to figure 1 for the wall-suction induced receptivity, we have magnified the $\Lambda_{wake}^{(r)}$ values by 100 before plotting to fit both curves on the same plot. However, unlike in figure 1, the qualitative shapes of both efficiency function curves are

seen as quite similar to each other. That is, both $\Lambda^{(r)}_{wake}$ and $\Lambda^{(r)}_{acoustic}$ are nearly zero at small values of f, and increase monotonically with f all the way to $f = 80 \times 10^{-6}$, which is the highest frequency considered in figure 4. Based on our previous discussion regarding the influence of wake position on the efficiency function, we may anticipate that the magnitude of $\Lambda^{(r)}_{wake}$ will decrease rapidly, especially at the larger frequencies in figure 4, when the parameter Y_c is increased beyond 5.0. Because the wave numbers α_{ins} and α_w are independent of the source of mean-flow disturbance, the extent of the above reduction will be exactly the same as that found in figure 2 for suction-induced receptivity.

Figure 4 shows that for $f = f_{lb}$, the magnitude of $\Lambda^{(r)}_{wake}$ is approximately 130 times smaller than the magnitude of $\Lambda^{(r)}_{acoustic}$. Although this ratio is much larger than the corresponding ratio (≈ 80) for the suction-induced receptivity, for typical values of the wall-suction velocity used in LFC systems (viz., $\epsilon^{(s)}_w = O(2 \times 10^{-4})$), comparable receptivity will be produced by roughness elements that correspond to $\epsilon^{(r)}_w \approx 1/55$. The linear theory was found to be accurate to $\epsilon^{(r)}_w = 1/6$ (at a comparable Reynolds number) in the acoustic case [29], [30]. If we assume a similar range of validity in the case of receptivity to a convected disturbance, then the above comparison implies that higher coupling coefficients may be obtained more easily (in an experiment) by using artificial surface humps than by increasing the suction level beyond $\epsilon^{(s)}_w = O(2 \times 10^{-4})$, because the latter will also reduce the overall amplification of the generated instability wave. For a rectangular roughness strip (with a height distribution $F^{(r)}(X)$ that is identical to eq. (6) with $\mathcal{V}_w = 1$) that corresponds to $\epsilon^{(r)}_w = 1/6$, a maximum coupling coefficient of 0.276 percent would be obtained at the lower branch frequency. The instability wave at this frequency is magnified by $\approx e^{6.2}$ by the time it reaches the upper branch location (where measurements are typically carried out [24]); therefore, the amplitude of the generated wave at the upper branch location is predicted to be 1.35 times the initial wake amplitude. Combined with a predicted increase by ≈ 8.9 when a periodic array of similar roughness strips is introduced, the measured TS-wave signal can be boosted to levels that are nearly 12 times larger than the wake amplitude. Not withstanding the other advantages of using a convected-wake disturbance (see Introduction), this appears to be a satisfactory level for accurate measurements of boundary-layer receptivity in an experiment.

We now demonstrate that the receptivity to convected wakes can be further increased a modest amount by introducing additional wake disturbances above the primary wake that is closest to the plate surface. In particular, we consider a semi-infinite array of equidistant wakes in which the first wake is centered at $Y = Y_c$, with a distance p (locally) between any pair of adjacent wakes. In this

case, equation (6) implies that the ratio of the efficiency function for the wake array to that for an individual wake centered at $Y = Y_c$ is given by

$$\frac{\Lambda^{(r)}_{wake\ array}}{\Lambda^{(r)}_{wake}} = \sum 1 + \xi_0 + \xi_0^2 + \xi_0^3 + \ldots \qquad \{\xi_0 = \exp\ [-p(\alpha_{ins} + \alpha_w)]\}\,. \tag{7}$$

The sum of the series on the right-hand side of (7) is equal to $1/(1 - \xi_0)$, which can be significant if the wake pitch p is considerably smaller than the local instability wavelength. If $p = 4$ is chosen (in conjunction with, say, $L = 1$), then the predicted increase in the efficiency-function magnitude at $f = f_{\mathrm{lb}}$ is about 55 percent for an entire array, although an increase of 35 percent can be obtained by placing just one additional wake. Higher increase is possible at lower frequencies; for example, receptivity can be more than doubled by introducing additional wakes at $f = 20 \times 10^{-6}$.

Considering the above results, we conclude that considerable variations in receptivity are possible depending on the form of the convected disturbance. However, with a proper design, an experiment is feasible that verifies the theoretically predicted features of receptivity to convected disturbances in the presence of short-scale surface nonuniformities. The convected wake model, in particular, appears promising from the standpoint of such an experiment.

Acknowledgements

Financial support for this work was provided by the Theoretical Flow Physics Branch at NASA Langley Research Center, Hampton, VA 23681, under contract NAS1-19299.

References

[1] Morkovin, M. V., "Critical Evaluation of Transition from Laminar to Turbulent Shear Layers with Emphasis on Hypersonically Traveling Bodies," AFFDL-TR-68-149, 1969.

[2] Reshotko, E., "Boundary layer stability and transition," *Ann. Rev. Fluid Mech.*, Vol. 8, pp. 311-349, 1976.

[3] Goldstein, M. E., "The Evolution of Tollmien-Schlichting Waves Near a Leading Edge," *J. Fluid Mech.*, Vol. 127, pp. 59-81, 1983.

[4] Goldstein, M. E., "Scattering of Acoustic Waves into Tollmien-Schlichting Waves by Small Streamwise Variations in Surface Geometry," *J. Fluid Mech.*, Vol. 154, pp. 509-529, 1985.

[5] Zavol'skii, N. A., Reutov V. P. and Ryboushkina, G. V., "Generation of Tollmien-Schlichting Waves via Scattering of Acoustic and Vortex Perturbations in Boundary Layer on Wavy Surface," *J. Appl. Mech. Techn. Physics*, pp. 79-86, 1983.

[6] Ruban, A. I., "On the Generation of Tollmien-Schlichting Waves by Sound," Transl. in *Fluid Dyn.*, Vol. 19, pp. 709-16, 1985.

[7] Fedorov, A. V., "Excitation and Development of Unstable Disturbances in Unstable Boundary Layers," Ph. D. Dissertation, Moscow Institute of Physics and Technology, 1982 (in Russian).

[8] Fedorov, A. V., and Zhigulev, V. N., "Boundary-Layer Receptivity to Acoustic Disturbances," *J. Appl. Mech. Techn. Physics*, Vol. 28, pp. 28-32, 1987.

[9] Kerschen, E. J., and Choudhari, M., "Boundary Layer Receptivity due to the Interaction of Free-Stream Acoustic Waves with Rapid Variations in Wall Suction and Admittance Distributions," *Bull. Am. Phys. Soc.*, Vol. 30, p. 1709, 1985.

[10] Goldstein, M. E. and Hultgren, L. S., "Boundary-layer Receptivity to Long-Wave Free-Stream Disturbances," *Ann. Rev. Fluid Mech.*, Vol. 21, pp. 138-166, 1989.

[11] Chen, C. F., ed., "Mechanics USA 1990," Proc. 11th US Natl. Cong. Appl. Mech., Tucson, Arizona, May 1990.

[12] Reda, D. C., Reed, H. L., and Kobayashi, R., eds., "Boundary Layer Stability and Transition to Turbulence," FED-Vol. 114, ASME, N.Y., 1991.

[13] Rogler, H., "The Coupling between Free-Stream Disturbances, Driver Oscillations, Forced Oscillations, and Stability Waves in a Spatial Analysis of a Boundary Layer," in *Laminar-Turbulent Transition*, AGARD CP-224, 1977.

[14] Kendall, J. M., "Studies on Laminar Boundary Layer Receptivity to Free-Stream Turbulence Near a Leading Edge," Boundary Layer Stability and Transition to Turbulence, ed. Reda et al., FED-Vol. 114, ASME, N.Y., pp. 17-22, 1991; see also: *Bull. Am. Phys. Soc.*, Vol. 36, No. 10, 1991, p. 2619.

[15] Rogler, H. and Reshotko, E., "Disturbances in a Boundary Layer Introduced by a Low-Intensity Array of Vortices," *SIAM J. Appl. Math.*, Vol. 28, No. 2, March 1975.

[16] Parekh, D., Pulvin, P. and Wlezien, R. W., "Boundary Layer Receptivity to Convected Gusts and Sound," Boundary Layer Stability and Transition to Turbulence, ed. Reda, D. C., Reed, H. L., and Kobayashi, R. K. et al., FED-Vol. 114, ASME, N.Y., pp. 69-75, 1991.

[17] Levchenko, V. Ya. and Kozlov, V. V., "Onset and Growth of Disturbances in a Boundary Layer," in *Models in Mechanics of Continuous Media*, [in Russian], *Izd. Teor. Prikl. Mekh.*, Sib. Otd. Akad. Nauk SSSR, Novosibirsk, 1979.

[18] Kerschen, E. J., "Linear and Non-Linear Receptivity to Vortical Free-Stream Disturbances," Boundary Layer Stability and Transition to Turbulence, ed. Reda, D. C., Reed, H. L., and Kobayashi, R. K. et al., FED-Vol. 114, ASME, N.Y., pp. 43-48, 1991.

[19] Crouch, J. D., "Nonlocalized Receptivity to Vortical Free-Stream Disturbances," *Instability, Transition and Turbulence*, M. Y. Hussaini, A. Kumar, and C. L. Streett, eds., Springer-Verlag, pp. 470-480, 1992.

[20] Heinrich, R. A. E., Choudhari, M., and Kerschen, E. J., "A Comparison of Boundary Layer Receptivity Mechanisms," AIAA-88-3758, presented at the 1st National Fluid Dynamics Congress, Cincinnati, Ohio, 1988.

[21] Buter, T. and Reed, H. L., "Numerical Investigation of Receptivity to Freestream Vorticity," AIAA Paper 93-0073, 1993.

[22] Parekh, D., "Receptivity of Boundary Layers to Convected Gusts," Rep. No. MDC 93B0041, prepared for US-AFOSR, Bolling Air Force Base, DC, 1993.

[23] Aizin, L. B. and Polyakov, M. F., "Acoustic Generation of Tollmien-Schlichting Waves over Local Unevenness of Surface Immersed in Stream (in Russian)," Preprint 17, Akad. Nauk USSR, Siberian Div., Inst. Theor. Appl. Mech., Novosibirsk, 1979.

[24] Saric, W., Hoos, J. A. and Radeztsky, R. H., "Boundary Layer Receptivity of Sound with Roughness," Boundary Layer Stability and Transition to Turbulence, ed. Reda, D. C., Reed, H. L., and Kobayashi, R. K. et al., FED-Vol. 114, ASME, N.Y., pp. 17-22, 1991.

[25] Wiegel, M. and Wlezien, R. W., "Acoustic Receptivity of Laminar Boundary Layers over Wavy Walls," AIAA Paper 93-3280, 1993.

[26] Wlezien, R. W., Parekh, D. E. and Island, T. C., "Measurement of Acoustic Receptivity at Leading Edges and Porous Strips," "*Mechanics USA 1990*," Chen, C. F., ed., Proc. 11th US Natl. Cong. Appl. Mech., Tucson, Arizona, pp. S167-S174, May 1990.

[27] Goldstein, M. E. and Hultgren, L. S., "A Note on the Generation of Tollmien-Schlichting Waves by Sudden Surface Curvature Change," *J. Fluid Mech.*, Vol. 181, pp. 519-525, 1987.

[28] Choudhari, M. and Streett, C. L., "Boundary Layer Receptivity Phenomena in Three-Dimensional and High-Speed Boundary Layers," AIAA Paper 90-5258, Oct. 1990.

[29] Choudhari, M. and Streett, C. L., "A Finite Reynolds Number Approach for the Prediction of Boundary Layer Receptivity in Localized Regions," NASA TM-102781, Jan. 1991 (also in *Phys. Fluids A*, Nov. 1992).

[30] Crouch, J. D., "Initiation of Boundary-Layer Disturbances by Nonlinear Mode Interactions," Boundary Layer Stability and Transition to Turbulence, ed. Reda et al., FED-Vol. 114, ASME, N.Y., pp. 63-68, 1991. (also in *Phys. Fluids A*, Jun. 1992)

[31] Choudhari, Meelan, "Boundary-Layer Receptivity due to Distributed Surface Imperfections of a Deterministic or Random Nature," *Theoretical and Computational Fluid Dynamics*, Vol. 4, No. 3, pp. 101-118, Feb. 1993 (also in NASA CR-4439, May 1992).

[32] Ryzhov, O., "Excitation of Unstable Oscillations in a Boundary Layer by a Source in the Potential in the Potential Flow Region," *Sov. Phys. Dok.* Vol. 34, No. 2, pp. 79-81, 1989.

[33] Choudhari, M., "Roughness-Induced Generation of Crossflow Vortices in Three-Dimensional Boundary Layers," *Theoretical and Computational Fluid Dynamics*, Vol. 6, No. 1, pp. 1-31, 1994 (also in NASA CR-4505, 1993).

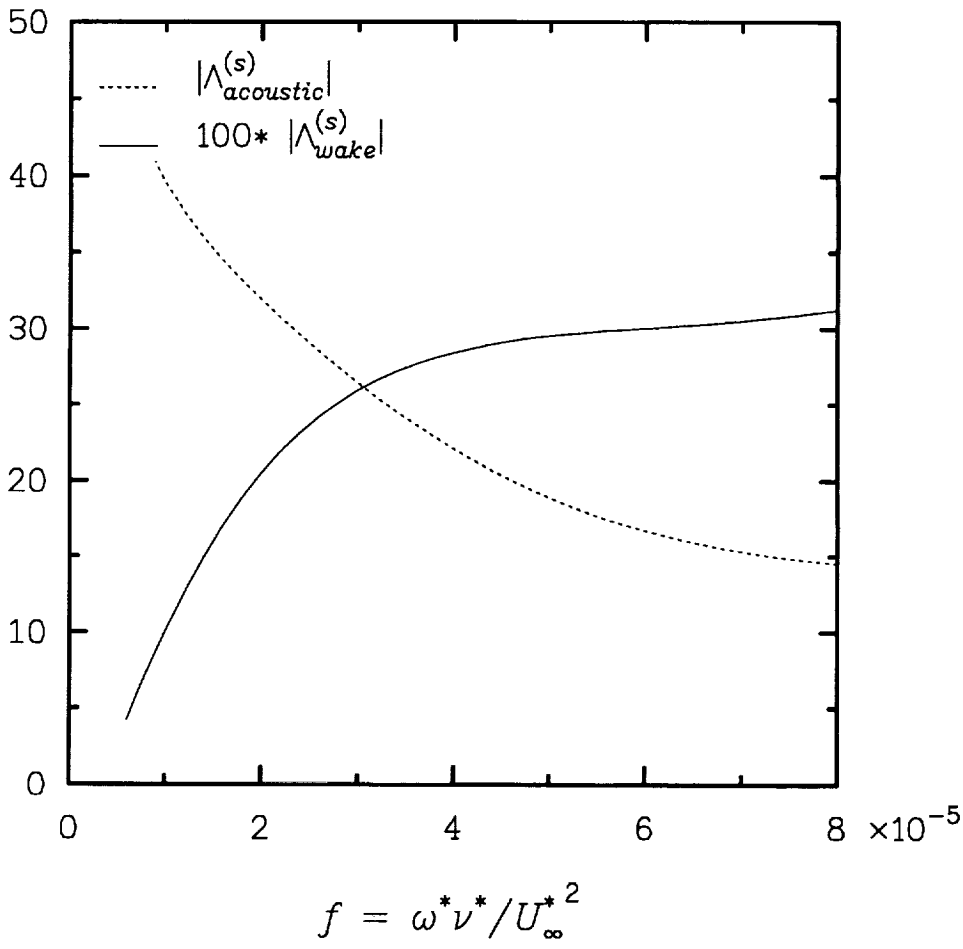

Figure 1. Variation in magnitudes of the efficiency functions $\Lambda^{(s)}_{wake}$ and $\Lambda^{(s)}_{acoustic}$ with $f=\omega^*\nu^*/U_\infty^{*2}$, while location of surface inhomogeneity is held fixed at R=700.

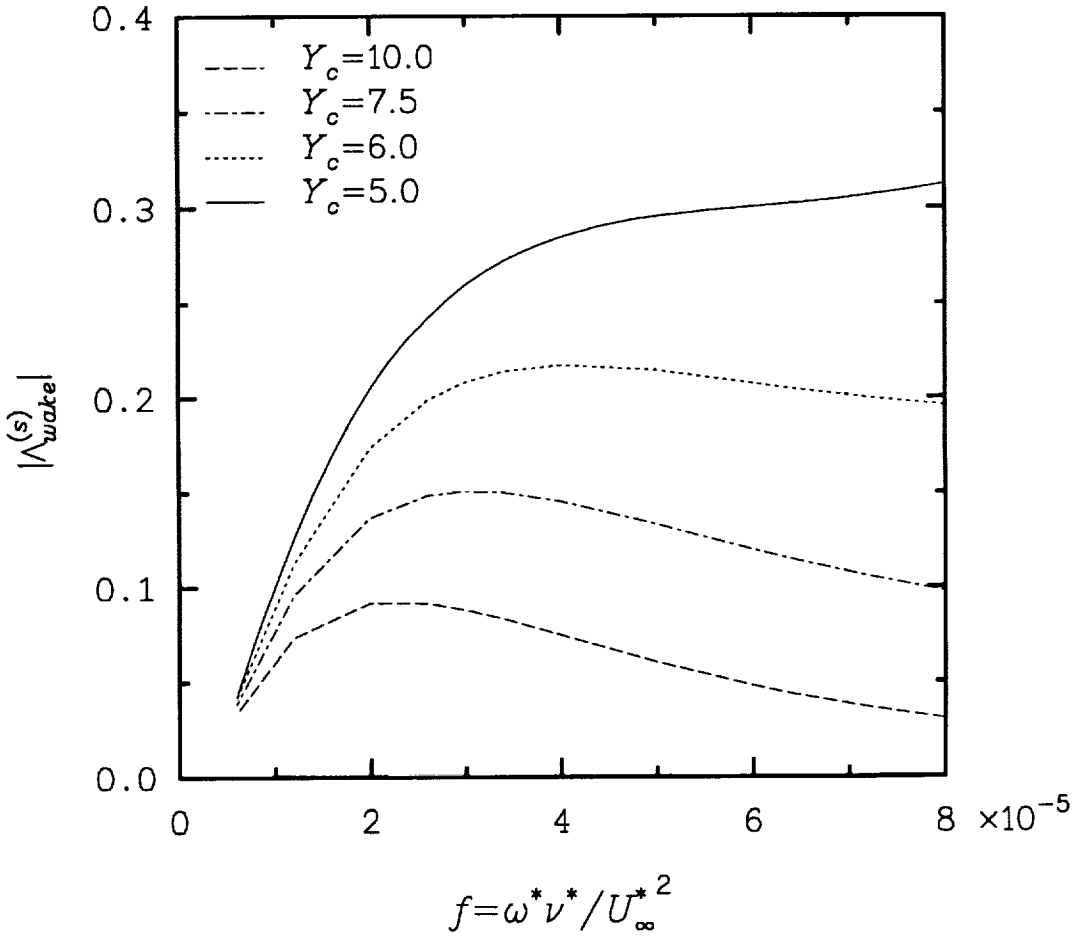

Figure 2. Influence of wake position on magnitudes of efficiency function $\Lambda^{(s)}_{wake}$. Location of surface inhomogeneity is held fixed at R = 700 while f is varied.

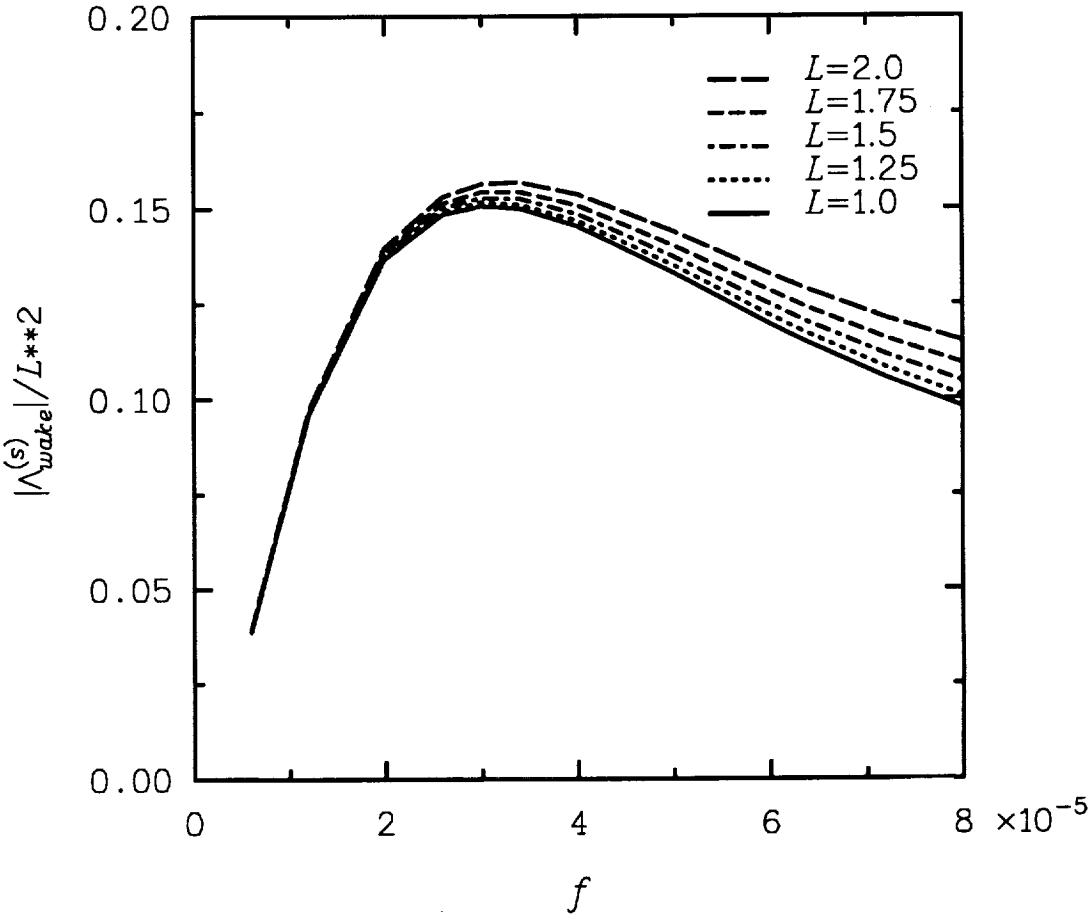

Fig. 3. Influence of wake width on magnitude of $\Lambda^{(s)}_{wake}$. Location of surface inhomogeneity is held fixed at R = 700, while f is varied. Wake-centerline position corresponds to Y_c=7.5.

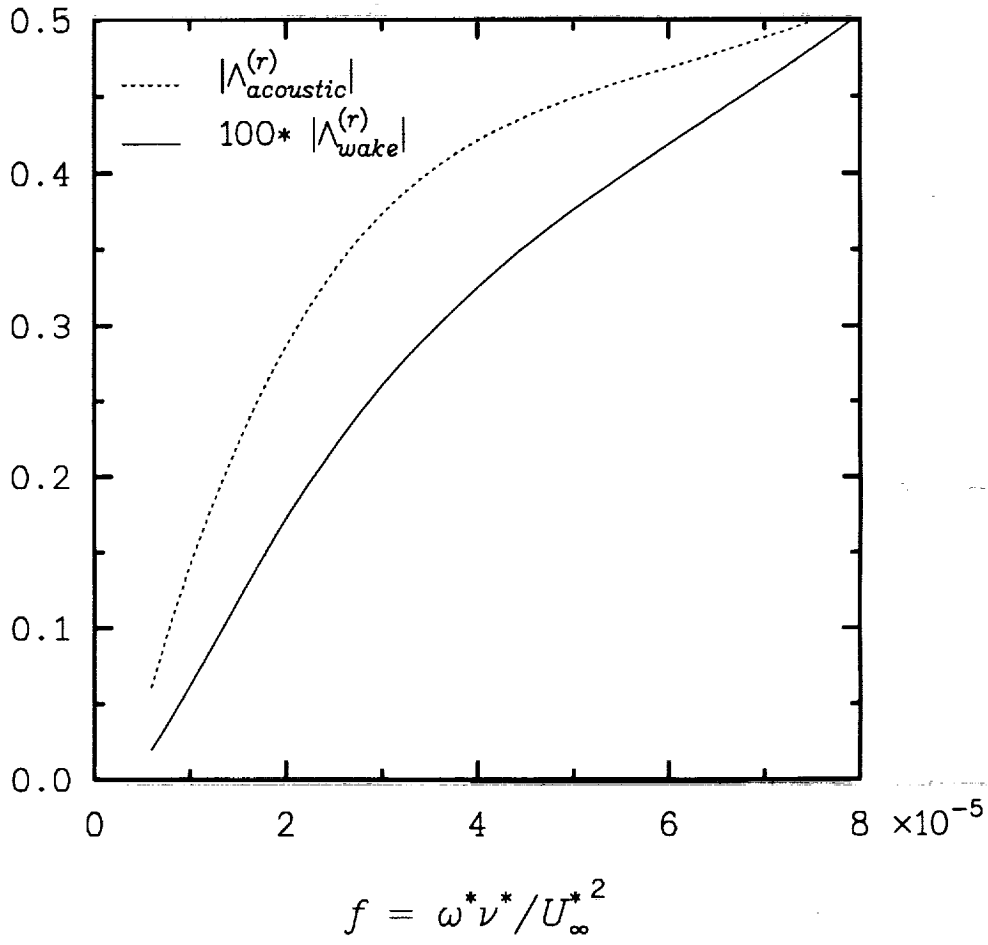

Figure 4. Variation in magnitudes of the efficiency functions $\Lambda^{(r)}_{wake}$ and $\Lambda^{(r)}_{acoustic}$ with $f=\omega^*\nu^*/U_\infty^{*2}$, while location of surface inhomogeneity is held fixed at R=700.

REPORT DOCUMENTATION PAGE

Form Approved
OMB No. 0704-0188

1. AGENCY USE ONLY (Leave blank)	2. REPORT DATE	3. REPORT TYPE AND DATES COVERED
	April 1994	Contractor Report

4. TITLE AND SUBTITLE
Localized and Distributed Boundary-Layer Receptivity to Convected Unsteady Wake in Free Stream

5. FUNDING NUMBERS
C NAS1-19299
WU 538-05-15-03

6. AUTHOR(S)
Meelan Choudhari

7. PERFORMING ORGANIZATION NAME(S) AND ADDRESS(ES)
High Technology Corporation
28 Research Drive
Hampton, VA 23666

8. PERFORMING ORGANIZATION REPORT NUMBER

9. SPONSORING/MONITORING AGENCY NAME(S) AND ADDRESS(ES)
National Aeronautics and Space Administration
Langley Research Center
Hampton, VA 23681-0001

10. SPONSORING/MONITORING AGENCY REPORT NUMBER
NASA CR-4578

11. SUPPLEMENTARY NOTES
Langley Technical Monitor: Craig L. Streett

12a. DISTRIBUTION/AVAILABILITY STATEMENT
Unclassified/Unlimited

Subject Category: 34

12b. DISTRIBUTION CODE

13. ABSTRACT *(Maximum 200 words)*

Receptivity to a model convected disturbance in the presence of localized and distributed variations in wall geometry and wall-suction velocity is examined. The model free-stream disturbance corresponds to the time-harmonic wake of a vibrating ribbon that is placed at a suitable distance above the surface of a thin airfoil. The advantages of using this disturbance for experiments on receptivity to convected disturbances are outlined. A brief parametric study is presented for a flat-plate boundary layer. The study quantifies the effect of wake position as well as wake width; in addition, it should be helpful in the choice of an optimal setting for a controlled experiment of the above type, which the above parametric study shows as feasible.

14. SUBJECT TERMS
boundary layers, receptivity, instability, transition, laminar flows, vorticity

15. NUMBER OF PAGES
22

16. PRICE CODE
A03

17. SECURITY CLASSIFICATION OF REPORT	18. SECURITY CLASSIFICATION OF THIS PAGE	19. SECURITY CLASSIFICATION OF ABSTRACT	20. LIMITATION OF ABSTRACT
Unclassified	Unclassified	Unclassified	Unlimited